Bioresource Technology 326 (2021) 124764

Contents lists available at ScienceDirect

Bioresource Technology

journal homepage: www.elsevier.com/locate/biortech

Role of extracellular polymeric substances and enhanced performance for biological removal of carbonaceous organic matters and ammonia from wastewater with high salinity and low nutrient concentrations

Wenchang Tang [a,b,1], Mengjie Wu [a,b,1], Wei Lou [c], Chunping Yang [a,b,c,d,*]

[a] Guangdong Provincial Key Laboratory of Petrochemcial Pollution Processes and Control, School of Environmental Science and Engineering, Guangdong University of Petrochemical Technology, Maoming, Guangdong 525000, China
[b] College of Environmental Science and Engineering, Hunan University, and Key Laboratory of Environmental Biology and Pollution Control (Hunan University), Ministry of Education, Changsha, Hunan 410082, China
[c] Hunan Provincial Environmental Protection Engineering Center for Organic Pollution Control of Urban Water and Wastewater, Changsha, Hunan 410001, China
[d] Maoming Engineering Research Center for Organic Pollution Control, Maoming, Guangdong 525000, China

HIGHLIGHTS

- EPS promoted COD and NH_4^+-N removal by 13.2%–33.8% and 27.8%–42.1% at 3.5% salinity.
- EPS protected major carbon-related enzymatic reaction under salinity stress.
- Tyrosine in EPS contributed most to mitigation of cytotoxicity from salinity.
- Salt inhibited ATP decomposition by impeding Na^+K^+-ATPase activity by 44.3%–57.7%.
- Models for calculation of COD and NH_4^+-N removal rate at 3.5% salinity were built.

ARTICLE INFO

Keywords:
EPS
Saline wastewater
Bioreactor
Enzymatic activity
Removal rate

ABSTRACT

The role of EPS in removal of carbonaceous organic matters and NH_4^+-N in simulated mariculture wastewater was examined at salinity of 0–3.5% in a multi-soil-layering bioreactor. Results showed that at 3.5% of salinity, the total activity of dehydrogenases (which were used to decompose carbonaceous organic matters) could be promoted by 13.2%–33.8% by EPS, increasing the removal rates of COD and NH_4^+-N by 13.2%–33.8% and 27.8%–42.1%, respectively. Besides, the activity of amylase in EPS was enhanced by 79.8%. However, reactions of some key enzymes such as acetate kinase and Na^+K^+-ATPase would not be accelerated by EPS, resulting in an inhibition of 44.3%–57.7% on energy gaining from ATP, and further inducing cytotoxicity. It was found that the glycolysis efficiency was promoted by 4.12%–59.3% in the presence of EPS, and glycolysis could also occur in EPS. Additionally, tyrosine was the main component in EPS to balance osmotic pressure.

1. Introduction

There is a growing demand on mariculture in China due to the increasing human seafood consumption. Investigation has shown that per capita consumption of seafood in China has increased by seven folds since 1978 (Fabinyi, 2016). It is estimated that China will account for 38% of global seafood consumption by 2030 (Fabinyi, 2016; World Bank, 2014). Therefore, pollution caused by mariculture seems inevitable as large volumes of mariculture wastewater have been discharged into marine environments each year (Davies et al., 2019). Rich in carbonaceous dissolved organic matters as well as nitrogenous and phosphorus compounds, mariculture wastewater increases the risk of eutrophication of seawaters (Gonzalez et al., 2019; Lang et al., 2020; Lin et al., 2020a; Liu et al., 2015). As a result, undesirable consequences including increased growth and biomass of algae, changes in biodiversity, and degraded marine water quality can occur (Hu et al., 2019; Luo

* Corresponding author at: Guangdong Provincial Key Laboratory of Petrochemcial Pollution Processes and Control, School of Environmental Science and Engineering, Guangdong University of Petrochemical Technology, Maoming, Guangdong 525000, China.
E-mail address: yangc@hnu.edu.cn (C. Yang).
[1] These authors contributed equally to this article.

https://doi.org/10.1016/j.biortech.2021.124764
Received 23 November 2020; Received in revised form 7 January 2021; Accepted 8 January 2021
Available online 22 January 2021

et al., 2014; Zhou et al., 2018). These deleterious effects have raised concerns in recent years.

Generally, the concentrations of COD, NH_4^+-N and TP in mariculture wastewater are 50–120 mg/L, 6–13 mg/L and 1–4 mg/L, respectively, and the salinity of which is about 3.5% (Fabinyi, 2016; World Bank, 2014). Utilizing conventional wastewater treatment technologies may be unable to efficiently remove these pollutants from mariculture wastewaters. On the one hand, physicochemical treatment techniques such as filtration, flocculation, and coagulation usually cannot remove nitrogen and phosphorus, while adsorption is limited by its high cost (Lin et al., 2020b; Liu et al., 2007; Monsalvo et al., 2011). On the other hand, biological treatment techniques such as membrane technology and trickling filters are negatively affected by high salinity of marine aquaculture wastewaters (Gomez et al., 2019). For example, it was reported that 30 g/L of NaCl reduced microbial diversity in sequencing batch biofilm reactor, which resulted from the inhibitory effect of salinity on cell activity (Wang et al., 2017).

Despite the impact of salinity, biological treatments are still the predominant way to purify marine aquaculture wastewaters because of their capacity of cost-effectively removing nitrogen and phosphorus (Chen et al., 2018). For instance, Chen et al. (2018) studied the effects of salinity on sequence batch reactor (SBR) and suggested that removal efficiency of COD, NH_4^+-N, TP was 55.8%, 63.0%, and 55.6% at NaCl concentration of 20 g/L, respectively. Besides, extracellular polymer substances (EPS) as an important part of cell are widely distributed on biofilms. Evidences have shown that 5%–9% of phosphorus was reserved in EPS and EPS could response to shock load of ZnO nanoparticles (Mu et al., 2012; Zhang et al., 2013).

In this context, a cost-effective bioreactor, namely, sequential vertical flow trickling filter and horizontal flow multi-soil-layering bioreactor (VFTF-HFMSL) was adopted to treat simulated mariculture wastewater with high salinity and low nutrient concentrations. Salinity ranging from 0 to 3.5% was set to investigate the role of EPS in the removal of COD and NH_4^+-N. Moreover, two removal models were established to predict the concentrations of COD and NH_4^+-N at different salinities. Most of all, potential effects of EPS on cytotoxicity and COD metabolism were elucidated on molecular level. This study would provide reference to efforts to mitigate the risk of mariculture wastewater pollution.

2. Materials and methods

2.1. Experimental system

The VFTF–HFMSL system was built for long-term experiment to investigate the treatment performance and relationship between EPS and carbonaceous organic matters and NH_4^+-N removal. The schematic diagram and specific description of the equipment could be found in studies of Tang et al. (2020) and Zhang et al. (2015). Two lidless acrylic boxes were filled with different media, working as VFTF and HFMSL respectively. The VFTF (length × width × height = 320 × 160 × 600 mm), with apertures at the bottom, was filled with gravel and zeolite (Jinyun, Zhejiang, China). The HFMSL (length × width × height = 1200 × 160 × 320 mm), contained an inlet pool, an outlet pool, and a MSL bioreactor. The MSL bioreactor consisted of six soil mixture block-layers that were surrounded by permeable layers in brick-like pattern. VFTF was equipped with zeolite, favoring microbial growth. Simulated wastewater was intermittently pumped from the storage tank into the system by a submersible pump (YQB-7500, Sensen Group Co. LTD., Zhoushan, Zhejiang, China) controlled by a time switch (DJ-D14M, Dingshibao, Shenzheng, China). The pumped water was evenly dispersed into the VFTF through a set of perforated pipes (R = 10 mm, PVC), and finally gravitated into the HFMSL.

Simulated mariculture wastewater was prepared by dissolving starch, NH_4Cl, KH_2PO_4, K_2HPO_4 (all reagents were analytically pure grade) into 40 L of tap water. The quality of the synthetic wastewater was in accordance with the actual water quality of mariculture wastewater (Fabinyi, 2016; World Bank, 2014). COD, NH_4^+-N and TP concentrations of the influent were 100, 10 mg/L and 3 mg/L throughout the whole long-term reaction and the NaCl concentration of the influent was gradually increased as 0, 0.5, 1, 2, 3.5%. The reactor ran at influent frequency of water feeding for 1 s per 8 min for about 12–20 days until contaminant indicators (COD, NH_4^+-N, NO_3^--N, NO_2^--N, TP) had become stable. The hydraulic loading rate (HLR) was kept at 660 L/m^2/d, and the corresponding nominal hydraulic retention time (HRT) was about 18 h.

Biofilm was taken from Changsha Guozhen Environmental Protection Technology Co., Ltd. Specific method of biofilm formation was shown in the article of Tang et al. (2020). The maximum, minimum and average ambient temperatures were 30.2 °C, 22.3 °C, and 24.6 °C, respectively. The maximum, minimum and average water temperatures were 23.2 °C, 16.4 °C, and 18.6 °C, respectively. These temperatures were suitable for biofilm living and growth, and could provide a relatively stable reaction environment.

Three water samples with volume of 50 mL of the influent, middle and final effluent were taken from the storage tank, the inlet pool in HFMSL, and the outlet pool in the HFMSL (Fig. 1), respectively. Water samples were collected and analyzed every 2 days. The concentration of NH_4^+-N was measured according to the standard methods (EPA of China, 2002), and COD was measured by high-chlorine wastewater – chlorine emendation method according to HJ/T 70-2001 (EPA of China, 2002). All reagents used in the test were in analytical pure grade.

2.2. Batch experiments

Biofilms in VFTF (BV) and biofilms in soil layer of HFMSL (BS), which were taken from zeolite in VFTF and soil in HFMSL (Fig. 1), respectively, were used to investigate the role of EPS in carbonaceous organic matter metabolism. Biofilm samples were taken at the end of each phase. In batch experiments, biofilm samples collected from every phase were divided in 3 groups, namely original biofilms, EPS-removed biofilms and EPS.

Totally 5 batch experiments according to 5 salinity concentrations were conducted within 24 h after biofilms were sampled. For instance, when VFTF-HFMSL system operated at the end of 0% salinity, the biofilms were sampled and separated into 3 groups (original biofilms, EPS-removed biofilms and EPS) was operated batch experiment. This was the first batch and the rest (biofilms taken from 0.5% to 3.5% salinity) operated in the same manner.

Original biofilms, EPS-removed biofilms and EPS were all pretreated in 0% and 3.5% saline buffer for 2 h. Specific buffer was according to the testing kits of enzymes. Carbonaceous organic matter metabolism related enzymes (dehydrogenases, amylase, acetate kinase, pyruvate kinase and Na^+K^+-ATPase) and cytotoxicity were tested after pretreatment. Ultrasonically separated EPS was detected by three-dimensional excitation emission matrix (3D-EEM) at the same time. Subsequently, samples were stored at −80.0 °C. Thermal separated EPS was detected after all the reactions were completed.

2.3. Analytical methods

2.3.1. Separation and three-dimensional fluorescence detection of EPS

EPS was extracted with 1 g of fresh biofilm added with 10 mL of ultrapure water (Tang et al., 2020). EPS samples were ultrasonically separated for 10 min and with power density of 3 kW/L at the frequency of 20 kHz (Yu et al., 2008). After that, EPS samples were evenly mixed by a vortex mixer at 3000 r/min for 1 min and then centrifugated at 4000 r/min for 10 min. Thermal separation of EPS was conducted in terms of the method introduced by Li and Yang (2007). The spectrum of 3D-EEM was measured by fluorescence spectroscopy (Fluoromax-4 Spectro-fluorometer, HORIBA Scientific, France) with a 450 W Xe arc lamp. Emission (Em) scans and excitation (Ex) wavelengths were

performed from 200 to 400 nm and 200 to 500 nm, respectively. Both Ex and Em were at 5 nm intervals as well as ultrapure water was recorded as the blank (Li and Yang, 2007). Test of 3D-EEM and content of EPS used all EPS samples and each sample has 4 parallel samples. Removal of the inner filter effect and PARAFAC analysis refers to previous studies (Chai et al., 2019; Murphy et al., 2013; Zhou et al., 2019).

2.3.2. Enzymatic activity of biofilms

The enzymatic activity of the original biofilms, the EPS removed biofilms and EPS were all determined. Ultrasonically separated method was used to separate EPS for testing enzymatic activity and this method could maintain the cell activity and enzyme activity in both EPS and cells. Acetate kinase, pyruvate kinase, dehydrogenases, amylase, Na^+K^+-ATPase were tested, and the cell activity (release of lactate dehydrogenase) at each salinity was also measured. Test methods for acetate kinase, dehydrogenases referred to previous studies (Chen et al., 2018; Wang et al., 2018). Testing kits produced by Nanjing Jiancheng were used to test amylase (C016-1-1), pyruvate kinase (A076-1-1) and Na^+K^+-ATPase (A070-2-2) and testing kit produced by Sigma was used to test cell activity (4744926001).

2.3.3. Other analytical methods

Volatile suspended solid (VSS) was measured according to standard methods (EPA of China, 2002). The content of protein and polysaccharides were detected by coomassie brilliant blue G-250 method and anthrone-sulfuric acid method with bovine serum albumin and glucose as standard solution, respectively, specific methods can be seen in the study of (Chen et al., 2018). All the reagents used were in analytical pure grade.

2.4. Statistical methods

All the experiments were carried out in triplicate, and all the calculated results were shown as mean ± SE (standard error). One-way ANOVA was performed to compare all data. Statistical analyses were conducted using SPSS 17.0 (SPSS, Chicago, IL, USA), with significance level $p < 0.05$. Principal components analysis (PCA) was performed by using Origin 2017 with PCA app, which was based on the data of the maximum fluorescence intensity from parallel factor analysis (PARAFAC) results. PARAFAC was measured by Matlab 2018.

3. Results and discussion

3.1. Role of EPS in enhanced removal of carbonaceous organic matters at salinity stress

Dehydrogenases was used to study the metabolic function on carbonaceous organic matters of the entire biofilm (Chen et al., 2018; Shi et al., 2019). As shown in Fig. 1a and b, the activity of dehydrogenases decreased with increase of salinity in biofilms. However, the dehydrogenases activity in original biofilms at 3.5% salinity was averagely 12.5% higher than that of 0% salinity. This indicated that salt would enable biofilms to decompose organic matters and gain more energy (Muhlbachova et al., 2015). Nonetheless, ability of biofilms to decompose carbonaceous organic matters would be significantly reduced under a long-term hypersaline condition. Results suggested that the decomposition efficiency of biofilms was decreased by 72.8% in BV and 81.8% in BS as salinity increased from 0% to 3.5%. Dehydrogenase activity in BS was higher than that in BV, which could be explained by two reasons. Firstly, most of the starch could not reach the HFMSL. Secondly, the major carbon source of BS was from the decomposition of sawdust in mixed soil which was more difficult to be decomposed.

From Fig. 1a and b, activity of dehydrogenases in EPS-removed biofilms (both BV and BS) was significantly inhibited in 3.5% saline buffer but was not obviously inhibited in 0% saline buffer. After being pretreated by 0% buffer, the activity of EPS-removed biofilms was unchanged compared with the original biofilms. However, after being pretreated by 3.5% buffer, the activity of EPS-removed biofilms was 11.0%–80.4% lower than the original biofilms. Besides, the difference in dehydrogenase activity between the original biofilms and EPS-removed biofilms decreased as the salinity increased. This demonstrated that salinity could damage EPS and EPS could promote the function of dehydrogenases pathway in salinity. Dehydrogenases represents a series of processes of carbonaceous organic matter metabolism (Muhlbachova et al., 2015), suggesting that EPS can promote the efficiency of carbonaceous organic matter usage rate with the presence of salt. This was one of the reasons why the system could maintain a high COD removal rate at 3.5% salinity (84.1%, in Fig. 5a). However, dehydrogenases, which was a general term for a series of enzymes, includes all enzymes in carbonaceous organic matter metabolism (Zhang et al., 2016). In this case, EPS may prevent most or all enzymes in the carbonaceous organic matter metabolism from being inhibited. In general, short-term increase in osmotic pressure would promote the activity of carbonaceous organic matters, but long-term exposure of biofilms to 3.5% of salinity would seriously inhibit it, and EPS could protect it from being inhibited.

3.2. Role of EPS in enhanced amylase activity at salinity stress

Since starch was the sole carbon source in this study, the activity of amylase needed to be investigated. It was reported that EPS might contain amylase (Cheng and Stomp, 2009; Tang et al., 2020), and the activity of amylase in EPS was also tested. As shown in Fig. 2a and b, the activity of amylase in BV increased when salinity increased, but the activity of amylase in BS remained stable and was lower than that of BV. This may be because that the highest COD in the middle effluent did not exceed 30 mg/L and starch was mainly consumed by BV. The activity of amylase at salinity of 3.5% was 79.8% higher than at salinity of 0%. In Fig. 2a, the activity of amylase in EPS increased with the increase of salinity and it seemed that the increase of amylase activity in BV mainly related to the amylase activity in EPS. The linear relationship between the amylase activity in EPS in BV and salinity was shown in the Fig. 2c, which illustrated that the amylase activity in EPS in BV was directly proportional to salinity. The scatter diagram was plotted by the amylase activity in BV as horizontal axis and amylase activity in EPS and biofilm without EPS removed as vertical axis as Fig. 2d. In Fig. 2d, the increase of the amylase activity in biofilms was only related to increase of the amylase activity in EPS in BV under the influence of salinity, indicating that the amylase in biofilms mainly produced by EPS. To conclude, starch could be more efficiently metabolized into glucose at salinity of 3.5%, and most of the metabolic pathways were located in EPS under salt conditions.

3.3. Effects of EPS on activity of glycolysis

It was shown that EPS could promote activity of glycolysis by 4.12%–59.3%. After starch is decomposed into glucose, it will enter the glycolysis pathway and produced pyruvate acid. Under anaerobic conditions, pyruvate acid is further metabolized to acetic acid (Sung et al., 2018; Tanja and Jorg, 2006). Therefore, the glycolysis pathway can be divided into production of pyruvate acid process and production of acetic acid process, reflecting by the activity of pyruvate kinase and acetate kinase, respectively (Wang et al., 2018).

EPS could promote the activity of pyruvate kinase. As seen in Fig. 3a and b, the activity of pyruvate kinase was detected in EPS, showing that complete glycolysis pathway could happen in EPS. This was in consistent with the report of Sung et al., (2018). Besides, the activity of pyruvate kinase in biofilms was decreased from 100% to 25.3% in BV and from 43.9% to 17.4% in BS with the increase of salinity from 0% to 3.5%, and the activity of pyruvate kinase in EPS also followed this variation pattern. This suggested that the glycolysis pathway was greatly inhibited in both cells and EPS with the presence of salinity. The decrease of pyruvic acid would reduce the ATP produced by the

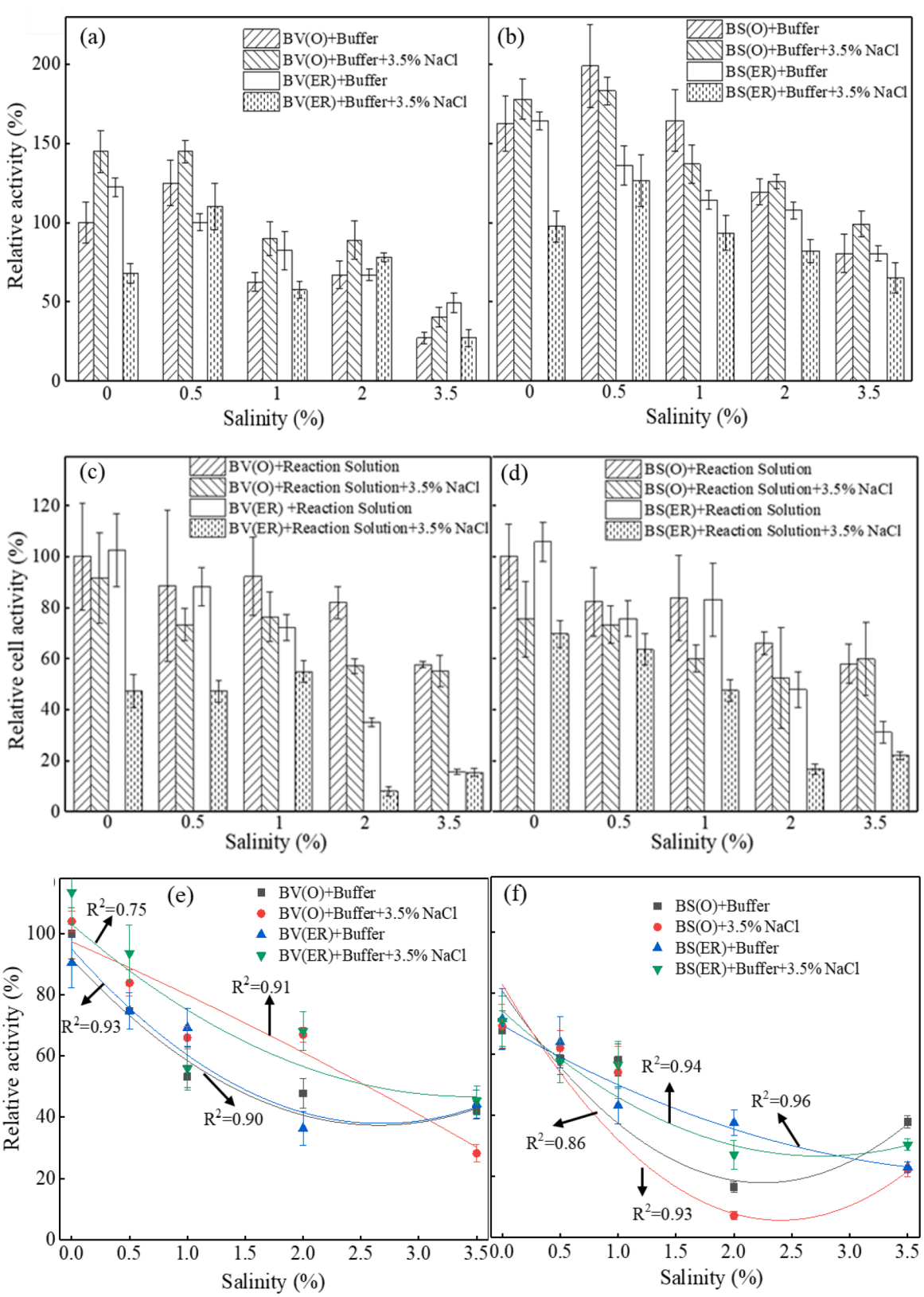

Fig. 1. Relative activity of dehydrogenases in biofilms. (a): BV; (b): BS. Cytotoxicity detection (releases of lactate dehydrogenase) after 1 h pretreatment under different Salinity. (c): BV; (d): BS. Relative activity of Na^+K^+-ATPase. (e): BV; (f): BS. ((O): original biofilms; (ER): EPS removed biofilms).

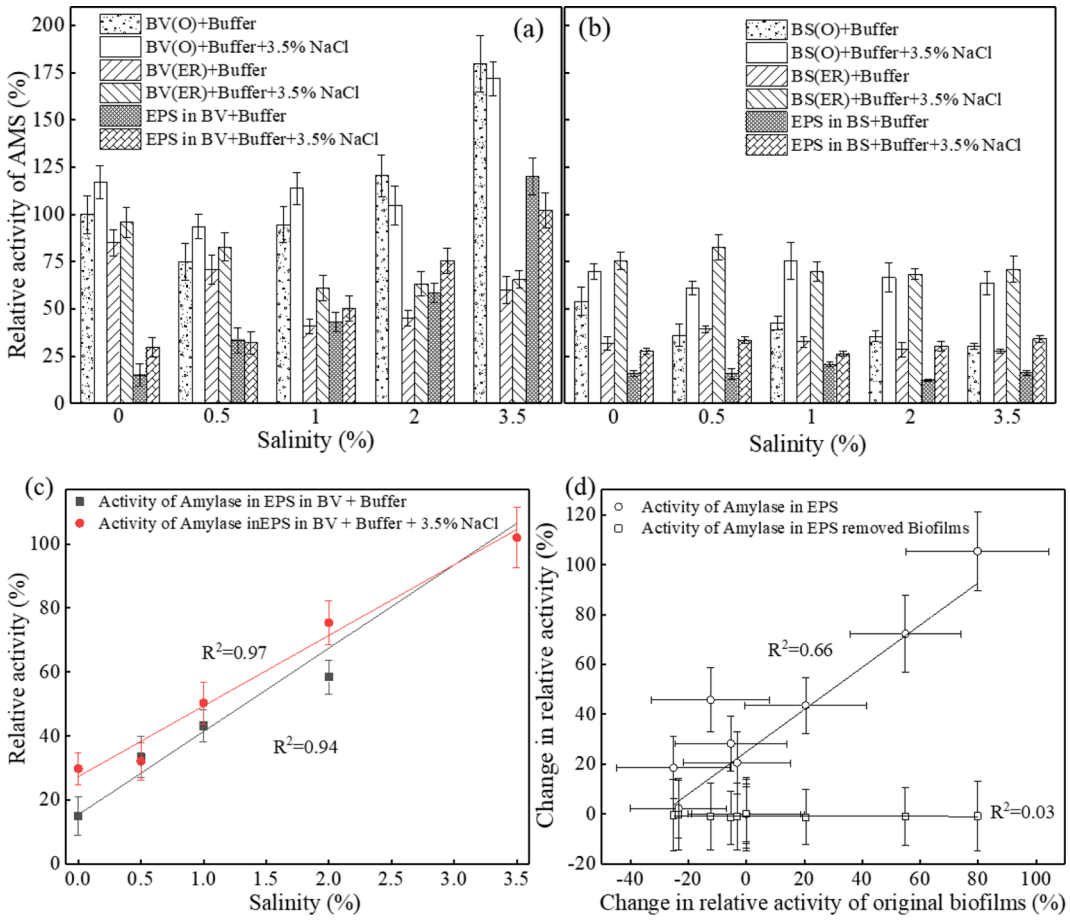

Fig. 2. Relative activity of amylase in biofilms and EPS. (a): BV; (b): BS. (c): Relative activity of amylase in EPS in BV; (d) Relationship of activity of amylase in original biofilms, EPS removed biofilms and EPS. ((O): original biofilms; (ER): EPS removed biofilms).

tricarboxylic acid cycle as well. In that way, biofilms could only obtain majority of ATP by secreting more amylases and this was the reason why the activity of amylase in BV was increased. Moreover, the activity of pyruvate kinase in original biofilms pretreated in 3.5% saline buffer was 5.17%–59.3% higher than that of EPS-removed biofilms. More importantly, only the activity of pyruvate kinase in the original biofilms increased after being pretreated by 3.5% saline buffer than that of 0% saline buffer, while the activity of pyruvate kinase in EPS-removed biofilms and EPS both decreased. This indicated that EPS could promote the process of glycolysis in both cells and EPS under the effects of salinity.

EPS only partly promoted the process of carbonaceous organic matter metabolism. In Fig. 3c and d, the activity of acetate kinase in BV was not inhibited by salinity, but was lower than BS. It was reported that HFMSL was mainly dominated by anaerobic environment while VFTF was aerobic (Tang et al., 2020). Acetate kinase activity was neither detected in EPS nor showed remarkable changes in biofilms after EPS was removed, which indicated that EPS did not have a protective effect on the acetate kinase pathway. Moreover, acetate kinase was one kind of dehydrogenases, which proved that EPS could prevent majority enzymes but not all enzymes in the carbonaceous organic matter metabolism from being inhibited.

3.4. Role of EPS in cytotoxicity of biofilms at salinity stress

Fig. 1c and d showed the activity of biofilms in VFTF-HFMSL system after 2 h pretreatment. In the pretreatment, the original biofilms and the EPS-removed biofilms were both placed in 0% and 3.5% saline buffer, respectively. The amount of lactate dehydrogenase released was tested after pretreatment for 2 h. As shown in Fig. 1c and d, the activity of biofilms was decreased with increase of salinity. After biofilms were taken from salinity of 0 ~ 2% in VFTF-HFMSL system with pretreatment in salinity of 3.5%, the activity of both the original and EPS-removed biofilms decreased significantly compared with being pretreated in salinity of 0% (Original biofilms: 8.33%–24.9% and 16.9 on average; EPS-removed biofilms: 12.1%–55.1% and 31.9% on average). This suggested that EPS could prevent cells from being inhibited by salinity. However, this phenomenon has not been observed in both the original and EPS-removed biofilms taken from salinity of 3.5% and the activity of biofilms taken from salinity of 2% and 3.5% did not increase after being pretreated at salinity of 0%. It indicated that salinity could cause irreparable damage to biofilms. On the other hand, the activity of EPS-removed biofilms was inhibited by 21.5%–49.1% in BV and 5.78%–37.8% in BS after being pretreated at 3.5% salinity compared with original biofilms. This showed that EPS played a significant role in osmotic pressure resistance (Han et al., 2017).

Although cell activity and glycolysis were severely impeded, the system had a high COD removal rate at salinity of 3.5% (84.1%, in Fig. 5a). Therefore, what was the most likely to directly cause cell inactivation was the suppression of Na^+K^+-ATPase, which is the end point of carbonaceous organic matter metabolism (Shi et al., 2019). Na^+K^+-ATPase is a kind of protein embedded in cell membrane (Han et al., 2017), whose role is to decompose ATP into ADP and free phosphorus and release high amount of energy (Zheng et al., 2017). In Fig. 1e and f, activity of Na^+K^+-ATPase was decreased with the increase of salinity in both BV and BS. Compared with salinity of 0%, the activity of Na^+K^+-ATPase in salinity of 3.5% was 42.3% and 55.7% in BV and in BS, respectively. This showed that salinity would dramatically inhibit the

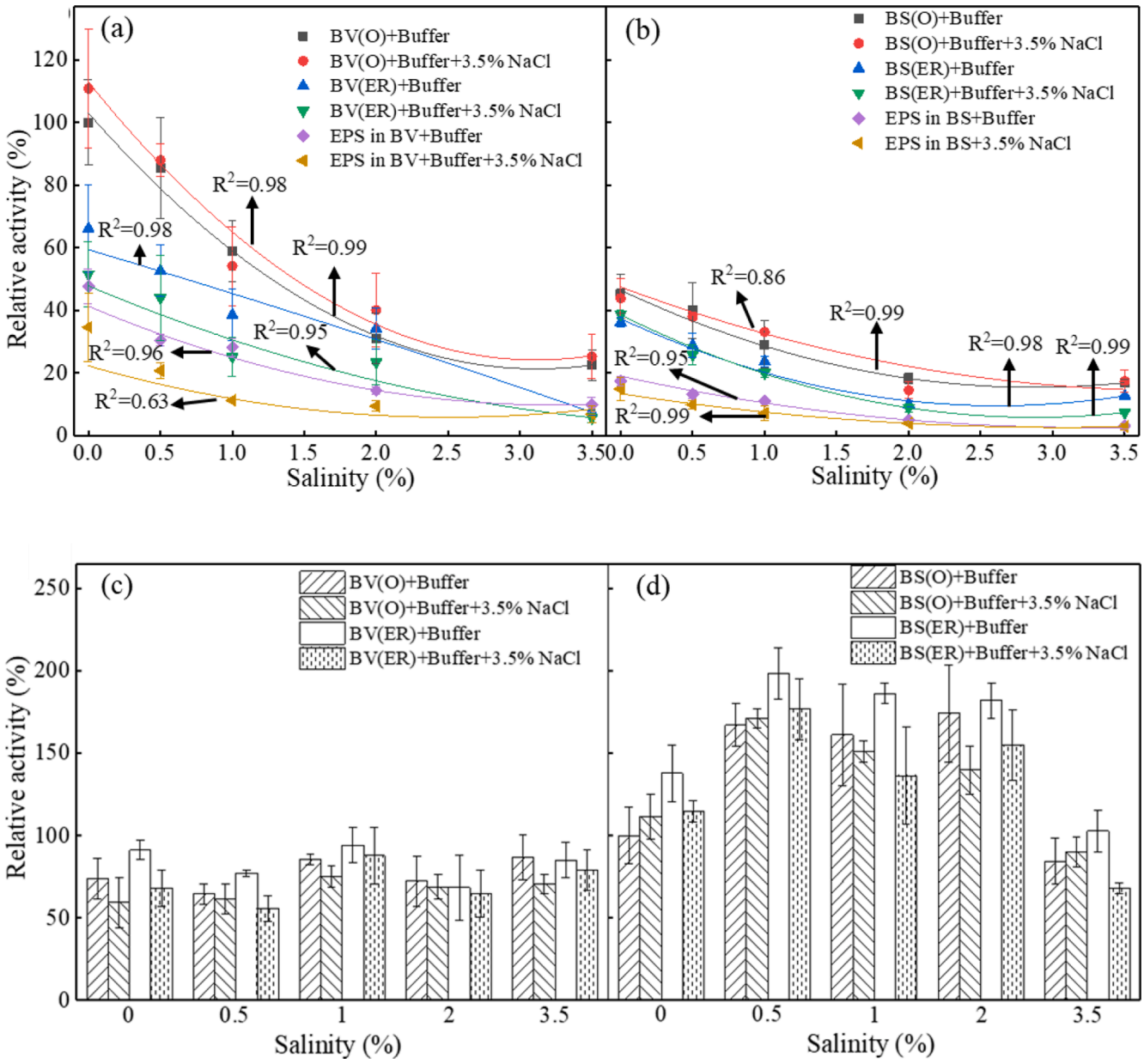

Fig. 3. Relative activity of Pyruvate kinase. (a): BV; (b): BS. Relative activity of Acetate kinase in biofilms. (c): BV; (d): BS. ((O): original biofilms; (ER): EPS removed biofilms).

decomposition of ATP and energy acquisition by cells. This directly resulted in the failure of cells to obtain enough energy to support various processes (Feng et al., 2018). In this case, the inhibition of Na^+K^+-ATPase was the most critical step leading to a decrease in the activity of the entire cell. In addition, from Fig. 1e and f, EPS cannot promote the progress of ATP metabolism.

3.5. Major components in EPS promoting enzymatic processes

The EEM spectra of EPS samples at different salinity were analyzed by PARAFAC. The results revealed that there were four components in EPS based on the split half analysis as well as residuals and loadings analysis. The first and second components both had two central peaks, which were located at Ex/Em = 275/330 and 220–230/330 nm, Ex/Em = 220/290 and 270/290 nm, respectively. The third component had three central peaks, which located at Ex/Em = 240/410, 280/410 and 340/410 nm, respectively. The fourth component was located at Ex/Em = 200–220/205–500 nm. Pure tyrosine was reported as two fluorescence peaks, which located at Ex/Em = 225/330 and 275/330 nm, respectively (Kowalczuk et al., 2009; Zhu et al., 2017). The peak of component 1 and pure tyrosine were overlapped, which indicated that component 1 was tyrosine. The study of Shutova et al. (2014) showed that the peak within Ex < 250 nm, Em = 320–360 nm and Ex/Em = 260–300/280–300 nm were all peaks of protein-like substance. The peak position of component 2 was included in protein-like substance, which indicated that component 2 was a kind of protein-like substances. It was reported that pure NADH had three peaks, which located at Ex/Em = 240/450, 280/450 and 340/450 nm (Wang et al., 2020; Zhou et al., 2019). The peaks of component 3 were 40 nm blue shifted compared with pure NADH (Wang et al., 2020), which indicated that component 3 was NADH-like substance. As humic-like substance usually located at Ex/Em = 200–260/400–500 nm (Ishii and Boyer, 2010; Zhou et al., 2019), suggesting that component 4 was humic-like substance.

According to the data of the maximum fluorescence intensity from PARAFAC results, the PCA analysis could be used to further study the change of the EPS of biofilms and four fluorescence components at

various salinity levels (Li et al., 2020a, 2020b, 2020c; Shutova et al., 2014). As shown in Fig. 4a, the EPS of BV was scatteredly and irregularly distributed, but the distribution was concentrated in a circle in BS. This suggested that the change in EPS of BV was greater than BS under the influence of salinity, which meant that EPS in BS was more suitable for salty environment compared with BV. In Fig. 4b, component 1 and 2 were scatteredly distributed, while component 3 and 4 were not the case, and component 3 was concentrated in a circle. This indicated that salinity mainly affected component 1 and 2 (tyrosine and protein-like substance) in EPS rather than components 3 and 4 (NADH-like substance and humic-like substance). Tyrosine has a significant antioxidant effect, and it could prevent the osmotic pressure from causing damage to cells, demonstrating that tyrosine was the main component in EPS to alleviate the influence of osmotic pressure (Bouthour et al., 2015; Kowalczuk et al., 2009). The major component of EPS was protein, and its content decreased with increase of salinity. This revealed that the protein in EPS might not have the function of alleviating the influence of osmotic pressure, and salt had a negative effect to the protein in EPS. In addition, although component 3 in the PCA graph did not have salient change, it was quenched at 3.5% salinity in BV. Nevertheless, component 3 was not quenched in BS at 3.5% salinity. This indicated that NADH-like substance may be quenched at 3.5% salinity in some kinds of microorganisms.

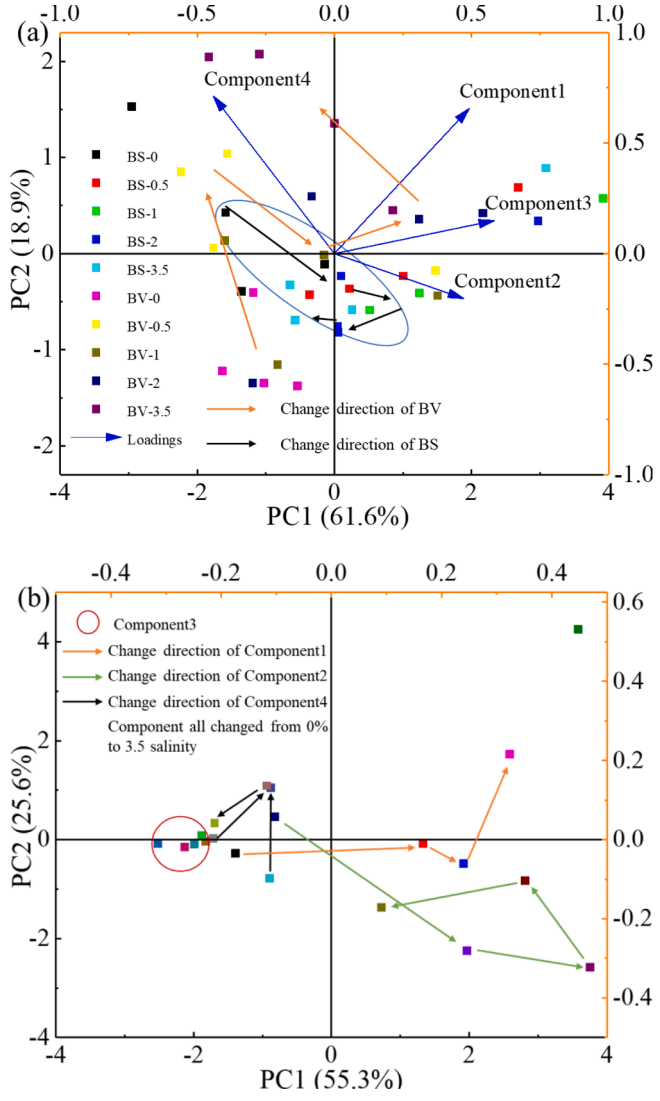

Fig. 4. PCA result based on the data of the maximum fluorescence intensity from PARAFAC result at 40 samples. (a): Biofilm samples; (b): Components.

3.6. Role of EPS in COD and NH_4^+-N removal at stress of salinity

In long-term reaction, EPS could not be removed through the whole reaction, and the carbonaceous organic matters were represented by COD. Under this condition, the role of EPS would be discussed by removal rate, removal model and enzymatic processes as discussed below. First of all, the VFTF-HFMSL system had a very high removal efficiency of COD and NH_4^+-N at low nutrients and salinity of 3.5%. Fig. 5a and c showed measured and model-predicted concentration of COD and NH_4^+-N, including the original synthetic wastewater, middle effluent, and final effluent at different salinities. As shown in Fig. 5a and c, the effluent concentration of COD, NH_4^+-N increased with the increase of salinity (0 ~ 3.5%). In this study, influent COD, NH_4^+-N and TP concentration were 100 ± 10.0, 10.0 ± 1.49 and 3 ± 0.63 mg/L, respectively. When salinity increased from 0 to 3.5%, middle and final effluent COD increased from 11.2 to 26.0 mg/L and from 1.76 to 15.87 mg/L, respectively. The removal rate of COD by the VFTF-HFMSL could stably reach 84.1% at salinity of 3.5% and initial concentration of 100 mg/L. Middle and final effluent of NH_4^+-N increased from 1.72 to 6.33 mg/L and from 0.12 to 4.14 mg/L as salinity increased from 0 to 3.5%. When salinity was 2% and 3.5%, the removal rate of NH_4^+-N by the system was 83.4% and 58.6%. This showed that salinity of 3.5% could greatly inhibit the removal efficiency of NH_4^+-N. In conclusion, VFTF-HFMSL system had promising removal efficiency on COD, NH_4^+-N at salinity of 3.5% at low nutrition condition. Since that EPS could promote the carbonaceous organic matters utility rate by 13.2%–33.8% at salinity of 3.5%, and the COD removal rate would decrease correspondingly in the absence of EPS. This indicated that EPS could promote COD removal rate under the influence of salinity. Moreover, modeling analysis would prove this conclusion and the decrease of COD removal rate would cause negative effects on NH_4^+-N removal.

3.7. Models for the relationship between COD/ NH_4^+-N removal and salinity

To find out the relationship between COD removal and salinity, modified logistic kinetic model (LKM) was used to fit stable COD effluent (Zhou et al., 2019), in which effluent concentration of COD was only related to salinity. The formula of modified LKM is:

$$\frac{dC}{dt} = -rC\left(1 - \frac{aC}{C_0}\right) \quad (1)$$

$$Q = 1 - \frac{aC}{C_0} \quad (2)$$

where C is COD concentration (mg/L), r is the removal rate constants (day^{-1}), C_0 is the initial amount of nutrient (mg/L), a is the parameter to be estimated ($a < 1$), Q is the external environmental stress.

In the VFTF-HFMSL system, due to the limitation of space, microorganisms grow slowly after acclimatization, r was set as 1. After inputting the data, the formulas could transfer to (COD-Middle: middle effluent of COD; COD-Final: final effluent of COD):

$$Q_{COD-Middle} = -0.0055NaCl^2 - 0.0027NaCl + 0.9412 \quad (3)$$

$$Q_{COD-Final} = 0.0009NaCl^2 - 0.0242NaCl + 0.991 \quad (4)$$

$$C_{COD-Middle} = 473.5e^{-Q_{COD-Middle}} - 174.25 \quad (5)$$

$$C_{COD-Final} = 497.12e^{-Q_{COD-Final}} - 182.77 \quad (6)$$

In the modified LKM, the parameter Q represents external environmental stress, and in this study the only external stress was salinity. Therefore, Q is only related to salinity, and also the stable value predicted by model.

Modified LKM and was used to fit stable COD effluent. Fig. 5a and b

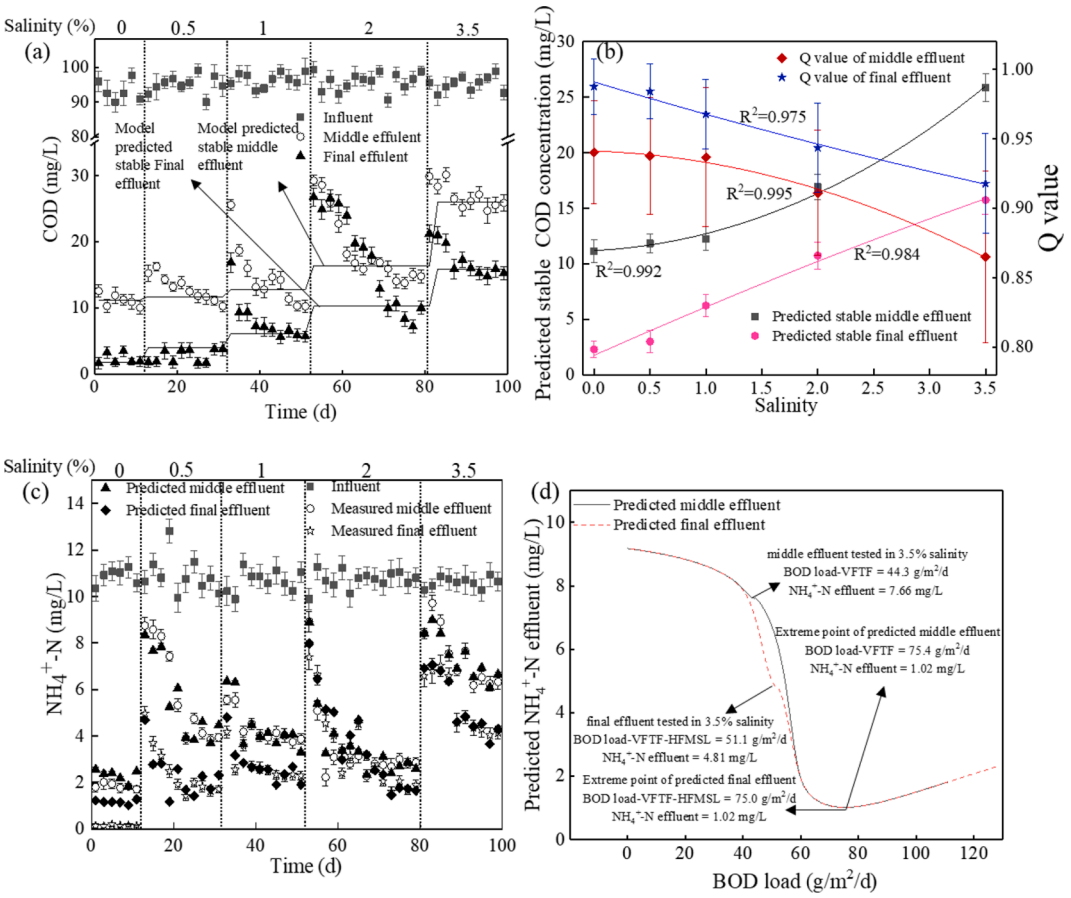

Fig. 5. (a): Removal performance and modified LKM predicted results of COD in VFTF-HFMSL system. (b): Stable COD effluent and Q value in various salinities; (c): Removal performance and modified PEM predicted results of NH_4^+-N in VFTF-HFMSL system; (d): Model of relationship between BOD load and NH_4^+-N effluent at salinity of 3.5%.

showed fitted curve of middle and final effluent of COD and Q value. In Fig. 5a, the prediction line basically coincided with the stable value of measured value. In Fig. 5b, the correlation coefficient (R^2) of Eqs. (3)–(6) was 0.995, 0.975, 0.992 and 0.984, respectively. This indicated that modified LKM was well fitted with COD effluent and Q value. The increase of COD effluent was related to salinity and could be described by salinity in VFTF-HFMSL system. Q value is an external environmental pressure index and Fig. 5b showed that Q value was related to salinity. This indicted that in this study, the only external environmental pressure was salinity and the COD removal was only related to salinity.

Modified LKM cannot be used to fit the NH_4^+-N effluent, which suggested that NH_4^+-N effluent was not affected by salinity. As a result, modified Pearce and Edwards model (PEM) was used to fit the NH_4^+-N concentration (Akker et al., 2011; Pearce and Edwards, 2011), in which effluent concentration of NH_4^+-N was only related to BOD load. The equation of modified PEM is:

$$C_{NH_4^+-NEffluent} = 0.00003*BODload^{2.06}*NH_4^+ - Nload^{3.04}*Iv^{-0.72}*T^{-0.24} - 0.0313*BODload^{1.03}*NH_4^+ - Nload^{1.52}*Iv^{-0.36}*T^{-0.12} + 9.1787 \quad (7)$$

where BOD load is g BOD/m^2 removed media surface area per day, NH_4^+-N load is g NH_4^+-N/m^2 removed media surface area per day, Iv is media irrigation rate specific to media surface area as L/m^2 media surface area per day, T is filter effluent temperature (℃).

In Fig. 5c, the majority of the predicted points of the model coincided with the actually measured points and R^2 of Eq. (7) and measured value was 0.94. In this model, effluent NH_4^+-N concentration was only related to BOD load but not salinity. However, modified PEM could be used well in salinity affected VFTF-HFMSL system in this study but modified LKM could not, which indicated that NH_4^+-N effluent was only related to BOD load.

NH_4^+-N removal rate would be seriously inhibited without EPS at salinity of 3.5%. Modified PEM was used to find the curve of BOD load and NH_4^+-N effluent concentration at salinity of 3.5%, which was showed in Fig. 5d. Since the variables in the model cannot be separated, an approximate solution was used to fit the NH_4^+-N effluent concentration at different BOD load in 3.5% salinity. Specific approximate solution is:

Firstly, the premise was assumed as: at salinity of 3.5%; the media irrigation rate and temperature did not change. In this case, both Iv and T are constants. Then the stable value of 3.5% salinity in this study was taken:

BOD_5 load = B_1; NH_4^+-N load = N_1

Inputting these two data into the Eq. (7) and obtain:

$C(NH_4^+\text{-}N_{Effluent}) = C_1$

And the equation for NH_4^+-N load in VFTF-HFMSL is

$$NH_4^+ - Nload = (NH_4^+ - N_{Influent} - NH_4^+ - N_{Effluent})*0.66 \quad (8)$$

When BOD_5 load increases by 1% as: BOD_5 load = B_2

At this time, assuming that the little change in BOD_5 load had little effect on NH_4^+-N effluent. In this case, C_1 was brought into Eq. (8) as an approximate value to obtain a new NH_4^+-N load, which could be set as N_2. N_2 and B_2 were brought into Eq. (7) to obtain C_2.

When BOD_5 load increased by 1% on the basis of B_2, which was set as B_3, C_2 was brought into Eq. (8) as an approximate value to get N_3 and then N_3, B_3 were brought into Eq. (7) to get C_3. The rest could be done in the same manner and the same as the BOD load was reduced.

As shown in Fig. 5d, when BOD load increased from 0 to 75.0 g/m^2/d (especially from 40.0 to 60.0 g/m^2/d), the effluent concentration of NH_4^+-N continuously decreased from 9.17 to 1.02 mg/L at salinity of 3.5%. This suggested that if the BOD load dropped from 60.0 to 40.0 g/m^2/d, the NH_4^+-N effluent would increase sharply. In this study, BOD loads were 51.1 (VFTF) and 44.3 (VFTF-HFMSL) g/m^2/d, which were both located in 40.0–60.0 g/m^2/d. If without the promotion function by EPS, which could promote BOD load by 13.2%–33.8% or 5.85–17.27 g/m^2/d in this study, the effluent concentration of NH_4^+-N would increase to 6.92–8.35 mg/L. The corresponding removal rate of NH_4^+-N decreased by 27.8%–42.1% at salinity of 3.5% when EPS was absent, which indicated that EPS could significantly promote the removal efficiency of NH_4^+-N.

3.8. A possible way to improve the removal efficiency of NH_4^+-N

In Fig. 5d, the optimal final effluent concentration of NH_4^+-N was 1.02 mg/L and the optimal BOD_5 load of the entire VFTF-HFMSL should be 75.0 g/m^2/d and corresponding C/N was COD: NH_4^+-N = 15: 1. In the experiments, this value was 51.1 g/m^2/d, showing that the COD concentration in the influent water could be increased by 46.8% to achieve the best nitrogen removal effect (89.8%). Of course, this was only the calculation by the model and was not verified in experiments. However, it also provided a possible solution to cost-effiective removal of NH_4^+-N in the treatment of marine aquaculture wastewater (high salinity and low nutritents). It was reported that carbon source metabolism was the basic activity of microorganisms (Oehmen et al., 2006), which directly affected the removal of nitrogen and phosphorus. This showed that it was feasible to increase BOD load, which could make microorganisms to absorb more carbon sources and to increase the removal rate of NH_4^+-N.

Appropriate carbon source should be selected among promoted enzymatic processes because of the promotion effects of EPS. The activity of amylase was promoted by 79.8% at salinity of 3.5% and the glycolysis pathway was inhibited by 16.9%–77.4%. This suggested that starch was better than glucose or other monosaccharides as substrate. Since the products of glycolysis were severely inhibited, the enzymatic activity in the subsequent tricarboxylic acid cycle would also decrease. However, the tricarboxylic acid cycle was the process that produced most of ATP, and the COD removal efficiency was very high at salinity of 3.5%. This indicated that acetic acid and pyruvate acid produced by glycolysis could be utilized mostly at tricarboxylic acid cycle and the remaining COD mainly consisted of glucose and leachable of cells. Therefore, the preferred external carbon source sequence for promoting removal of NH_4^+-N in the treatment of marine aquaculture wastewater should be starch > pyruvate acid > glucose.

4. Conclusions

EPS could distinctively protect enzymes in carbonaceous organic matters (such as amylase and pyruvate kinase), and tyrosine was main active component in EPS. Besides, salinity could inhibit the consumption of ATP and directly reduce the energy available to microorganisms. Moreover, VFTF-HFMSL system showed a high removal efficiency of COD at 3.5% salinity. The modified PEM predicted a highest NH_4^+-N removal efficiency of 89.8% (with the NH_4^+-N concentration in the effluent of 1.02 mg/L) at BOD_5 load of 75 g/m^2/d, and the optimal C/N of 15:1 (COD: NH_4^+-N), suggesting its potential application in adjusting C/N to achieve better NH_4^+-N removal performance.

CRediT authorship contribution statement

Wenchang Tang: Conceptualization, Methodology, Software, Validation, Formal analysis, Investigation, Writing - original draft, Project administration. **Mengjie Wu:** Methodology, Conceptualization, Validation, Formal analysis, Investigation. **Wei Lou:** Methodology, Investigation, Resources. **Chunping Yang:** Conceptualization, Validation, Investigation, Resources, Funding acquisition, Project administration.

Declaration of Competing Interest

The authors declare that they have no known competing financial interests or personal relationships that could have appeared to influence the work reported in this paper.

Acknowledgments

This work was supported by the National Natural Science Foundation of China (Grant No.: 51978178, 51478172 and 51521006), the Department of Science and Technology of Guangdong Province of China (Contract No.: 2019A1515012044), Maoming Municipal Bureau of Science and Technology of Guangdong Province of China (Contract No.: 2018S0013), the International S&T Cooperation Program of China (Contract No.: 2015DFG92750), and Guangdong University of Petrochemical Technology.

Appendix A. Supplementary data

Supplementary data to this article can be found online at https://doi.org/10.1016/j.biortech.2021.124764.

References

Akker, B.V.D., Holmes, M., Pearce, P., Cromar, N.J., Fallowfield, H.J., 2011. Structure of nitrifying biofilms in a high-rate trickling filter designed for potable water pretreatment. Water Res. 45, 3489–3498.

Bouthour, D., Kalai, T., Gouia, H., Chaffei, H.C., 2015. Biochemical and physiological changes in response to salinity in leaves and roots of two Durum wheat (*Triticum durum* Desf.) genotypes. Int. J. Adv. Res. 3, 1308–1319.

Chai, L.W., Huang, M.K., Fan, H., Wang, J., Jiang, D.L., Zhang, M.J., Huang, Y., 2019. Urbanization altered regional soil organic matter quantity and quality: Insight from excitation emission matrix (EEM) and parallel factor analysis (PARAFAC). Chemosphere 220, 249–258.

Chen, Y.J., He, H.J., Liu, H.Y., Li, H.R., Zeng, G.M., Xia, X., Yang, C.P., 2018. Effect of salinity on removal performance and activated sludge characteristics in sequencing batch reactors. Bioresour. Technol. 249, 890–899.

Cheng, J.J., Stomp, A.M., 2009. Growing duckweed to recover nutrients from wastewaters and for production of fuel ethanol and animal feed. Clean-Soil Air Water 37, 17–26.

Davies, I.P., Carranza, V., Froehlich, H.E., Gentry, R.R., Kareiva, P., Halpern, B.S., 2019. Governance of marine aquaculture: pitfalls, potential, and pathways forward. Mar. Policy 104, 29–36.

EPA of China, 2002. Water and Wastewater Monitoring Analysis Method, fourth ed. Chinese Environment Science Press, Beijing.

Fabinyi, M., 2016. Sustainable seafood consumption in China. Mar. Policy 74, 85–87.

Feng, Y., Zhao, Y.P., Guo, Y.Z., Liu, S.T., 2018. Microbial transcript and metabolome analysis uncover discrepant metabolic pathways in autotrophic and mixotrophic anammox consortia. Water Res. 128, 402–411.

Gomez, S., Hurtado, C.F., Orellana, J., 2019. Bioremediation of organic sludge from a marine recirculating aquaculture system using the polychaete *Abarenicola pusilla* (Quatrefages, 1866). Aquaculture 507, 377–384.

Gonzalez, G.L., Krah, D., Ghattas, A.K., Carballa, M., Wick, A., Helmholz, L., Lema, J.M., Ternes, T.A., 2019. Biotransformation of organic micropollutants by anaerobic sludge enzymes. Water Res. 152, 202–214.

Han, X.M., Wang, Z.W., Chen, M., Zhang, X.R., Tang, C.Y.Y., Wu, Z.C., 2017. Acute responses of microorganisms from membrane bioreactors in the presence of NaOCl: protective mechanisms of extracellular polymeric Substances. Environ. Sci. Technol. 51, 3233–3241.

Hu, H., Zhou, Q., Li, X., Lou, W., Du, C., Teng, Q., Zhang, D.M., Liu, H.Y., Zhong, Y.Y., Yang, C.P., 2019. Phytoremediation of anaerobically digested swine wastewater contaminated by oxytetracycline via *Lemna aequinoctialis*: Nutrient removal, growth characteristics and degradation pathways. Bioresour. Technol. 291, 121853.

Ishii, S.K., Boyer, T.H., 2010. Behavior of reoccurring PARAFAC components in fluorescent dissolved organic matter in natural and engineered systems: a critical review. Environ. Sci. Technol. 46, 2006–2017.
Kowalczuk, P., Durako, M.J., Young, H., Kahn, A.E., Cooper, W.J., Gonsior, M., 2009. Characterization of dissolved organic matter fluorescence in the South Atlantic Bight with use of PARAFAC model: interannual variability. Mar. Chem. 113, 182–196.
Lang, Z.C., Zhou, M.H., Zhang, Q.Z., Yin, X.Y., Li, Y.W., 2020. Comprehensive treatment of marine aquaculture wastewater by a cost-effective flow-through electro-oxidation process. Sci. Total Environ. 722, 137812.
Li, J.C., Wang, L.Y., Geng, J.J., Li, S.G., Yu, Q.M., Xu, K., Ren, H.Q., 2020a. Distribution and removal of fluorescent dissolved organic matter in 15 municipal wastewater treatment plants in China. Chemosphere 251, 126375.
Li, X., Yang, C.P., Zeng, G.M., Wu, S.H., Lin, Y., Zhou, Q., Lou, W., Du, C., Nie, L.J., Zhong, Y.Y., 2020b. Nutrient removal from swine wastewater with growing microalgae at various zinc concentrations. Algal Res. 46, 101804.
Li, X., Wu, S.H., Yang, C.P., Zeng, G.M., 2020c. Microalgal and duckweed based constructed wetlands for swine wastewater treatment: a review. Bioresour. Technol. 318, 123858.
Li, X.Y., Yang, S.F., 2007. Influence of loosely bound extracellular polymeric substances (EPS) on the flocculation, sedimentation and dewaterability of activated sludge. Water Res. 41 (5), 1022–1030.
Lin, Y., Yang, C.P., Wu, S.H., Li, X., Chen, Y.J., Yang, W.L., 2020a. Construction of built-in electric field within silver phosphate photocatalyst for enhanced removal of recalcitrant organic pollutants. Adv. Funct. Mater. 30 (38), 2002918.
Lin, Y., Liu, H.Y., Yang, C.P., Wu, X., Du, C., Jiang, L.M., Zhong, Y.Y., 2020b. Gama-graphyne as photogenerated electrons transfer layer enhances photocatalytic performance of silver phosphate. Appl. Catal. B: Environ. 264, 118479.
Liu, C.C.K., Xia, W., Park, J.W., 2007. A wind-driven reverse osmosis system for aquaculture wastewater reuse and nutrient recovery. Desalination 202, 24–30.
Liu, S., Chen, H., Xu, X.R., Liu, S.S., Sun, K.F., Zhao, J.L., Ying, G.G., 2015. Steroids in marine aquaculture farms surrounding Hailing Island, South China: occurrence, bioconcentration, and human dietary exposure. Sci. Total Environ. 502, 400–407.
Luo, W., Yang, C.P., He, H.J., Zeng, G.M., Yan, S., Cheng, Y., 2014. Novel two-stage vertical flow biofilter system for efficient treatment of decentralized domestic wastewater. Ecol. Eng. 64, 415–423.
Monsalvo, V., Mohedano, A., Rodriguez, J., 2011. Activated carbons from sewage sludge application to aqueous-phase adsorption of 4-chlorophenol. Desalination 277, 377–382.
Mu, H., Zheng, X., Chen, Y.G., Chen, H., Liu, K., 2012. Response of anaerobic granular sludge to a shock load of zinc oxide nanoparticles during biological wastewater treatment. Environ. Sci. Technol. 46, 5997–6003.
Muhlbachova, G., Sagova-Mareckova, M., Omelka, M., Szakova, J., Tlustos, P., 2015. The influence of soil organic carbon on interactions between microbial parameters and metal concentrations at a long-term contaminated site process. Sci. Total Environ. 502, 218–223.
Murphy, K.R., Stedmon, C.A., Graeber, D., Bro, R., 2013. Fluorescence spectroscopy and multi-way techniques. PARAFAC Anal. Methods 5, 6557–6566.
Oehmen, A., Zeng, J.R., Saunders, M.A., Blackall, L.L., Keller, J., Yuan, Z.G., 2006. Anaerobic and aerobic metabolism of glycogen-accumulating organisms selected with propionate as the sole carbon source. Microbiol. 152, 2767–2778.
Pearce, P., Edwards, W., 2011. A design model for nitrification on structured cross flow plastic media trickling filters. Water Environ. J. 25, 257–265.
Shutova, Y.L., Baker, A., Bridgeman, J., Henderson, R.K., 2014. Spectroscopic characterisation of dissolved organic matter changes in drinking water treatment: from PARAFAC analysis to online monitoring wavelengths. Water Res. 54, 159–169.
Shi, S.N., Liu, J.X., Xu, J., Zeng, Q.Z., Hou, Y., Jiang, B., 2019. Effects of biochar on the phenol treatment performance and microbial communities shift in sequencing batch reactors. Water Res. 161, 1–10.
Sung, T.O., Kang, S.J., Azizi, A., 2018. Electrochemical communication in anaerobic digestion. Chem. Eng. J. 353, 878–889.
Tang, W.C., Li, X., Liu, H.Y., Wu, S.H., Zhou, Q., Du, C., Teng, Q., Zhong, Y.Y., Yang, C.P., 2020. Sequential vertical flow trickling filter and horizontal flow reactor for treatment of decentralized domestic wastewater with sodium dodecyl benzene sulfonate. Bioresour. Technol. 300, 122634.
Tanja, R.W., Jorg, E.D., 2006. Using soil biomass as an indicator for the biological removal of effluent-derived organic carbon during soil infiltration. Water Res. 40, 961–968.
Wang, C.Q., Wang, C., Liu, J.Y., Xu, Q.J., Han, Z.X., Xu, X.Y., Zhu, L., 2020. Tolerance of aceticlastic methanogenesis enhanced by magnetite under the condition of ammonia stress. ACS Sustain. Chem. Eng. 8, 1417–1426.
Wang, D.B., Duan, Y.Y., Yang, Q., Liu, Y.W., Ni, B.J., Wang, Q.L., Zeng, G.M., Li, X.M., Yuan, Z.G., 2018. Free ammonia enhances dark fermentative hydrogen production from waste activated sludge. Water Res. 133, 272–281.
Wang, J., Gong, B., Huang, W., Wang, Y., Zhou, J., 2017. Bacterial community structure in simultaneous nitrification, denitrification and organic matter removal process treating saline mustard tuber wastewater as revealed by 16S rRNA sequencing. Bioresour. Technol. 228, 31–38.
World Bank. Fish to 2030: Prospects for Fisheries and Aquaculture; Agriculture and Environment Services Discussion Paper 3; World Bank Report number 83177-GLB; The World Bank: Washington, DC, USA, 2014.
Yu, G.H., He, P.J., Shao, L.M., Zhu, Y.S., 2008. Extracellular proteins, polysaccharides and enzymes impact on sludge aerobic digestion after ultrasonic pretreatment. Water Res. 42, 1925–1934.
Zhang, H.L., Fang, W., Wang, Y.P., Sheng, G.P., Zeng, J.R., Li, W.W., Yu, H.Q., 2013. Phosphorus removal in an enhanced biological phosphorus removal process: roles of extracellular polymeric substances. Environ. Sci. Technol. 47, 11482–11489.
Zhang, Y., Cheng, Y., Yang, C.P., Luo, W., Zeng, G.M., Lu, L., 2015. Performance of system consisting of vertical flow trickling filter and horizontal flow multi-soil-layering reactor for treatment of rural wastewater. Bioresour. Technol. 193, 424–432.
Zhang, Y., Li, B., Xu, R.X., Wang, G.X., Zhou, Y., Xie, B., 2016. Effects of pressurized aeration on organic degradation efficiency and bacterial community structure of activated sludge treating saline wastewater. Bioresour. Technol. 222, 182–189.
Zheng, X.Y., Lu, D., Chen, W., Gao, Y.J., Zhou, G., Zhang, Y., Zhou, X., Jin, M.Q., 2017. Response of aerobic granular sludge to the long-term presence of CuO NPs in A/O/A SBRs: Nitrogen and phosphorus removal, enzymatic activity, and the microbial community. Environ. Sci. Technol. 51, 10503–10510.
Zhou, Q., Lin, Y., Li, X., Yang, C.P., Han, Z.F., Zeng, G.M., Lu, L., He, S.Y., 2018. Effect of zinc ions on nutrient removal and growth of *Lemna aequinoctialis* from anaerobically digested swine wastewater. Bioresour. Technol. 249, 457–463.
Zhou, Q., Li, X., Lin, Y., Yang, C.P., Tang, W.C., Wu, S.H., Li, D.H., Luo, W., 2019. Effects of copper ions on removal of nutrients from swine wastewater and on release of dissolved organic matter in duckweed systems. Water Res. 158, 171–181.
Zhu, G.C., Bian, Y.N., Hursthouse, A.S., Wan, P., Szymanska, K., Ma, J., Wang, X.F., Zhao, Z.L., 2017. Application of 3-D fluorescence: characterization of natural organic matter in natural water and water purification systems. J. Fluoresc. 27, 1–26.